CBPF-NF-022/04

Half-life predictions for decay modes of superheavy nuclei

S. B. Duarte, O. A. P. Tavares

Centro Brasileiro de Pesquisas Físicas - CBPF/MCT
R. Dr. Xavier Sigaud 150, 22290-180, Rio de Janeiro, Brazil

M. Gonçalves

Instituto de Radioproteção e Dosimetria IRD/CNEN
Av. Salvador Allende s/n, 22780-160, Rio de Janeiro, Brazil

O. Rodríguez, F. Guzmán

Instituto Superior de Tecnologias y Ciencias Aplicadas - InSTEC
Av. Salvador Allende y Luaces, Apartado Postal 6163, La Habana, Cuba

T. N. Barbosa, F. García, A. Dimarco

Departamento de Ciências Exatas e Tecnológicas,
Universidade Estadual de Santa Cruz
Rod. Ilhéus-Itabuna, Km 16, 45650-000 Ilhéus-Ba, Brazil

We applied the Effective Liquid Drop Model (ELDM) to predict the alpha-decay, cluster emission and cold fission half-life-values of nuclei in the region of Superheavy Elements (SHE). The present calculations have been made in the region of the ZN-plane defined by $155 \leq N \leq 220$ and $110 \leq Z \leq 135$. Shell effects are included via the Q-value of the corresponding decay case. We report the results of a systematic calculation of the half-life for the three nuclear decay modes in a region of the ZN-plane where superheavy elements are expected to be found. Results have shown that, among the decay modes investigated here, the alpha decay is the dominant one, i. e. the decay mode of smallest half-lives. Half-life predictions for alpha decay, cluster emission and cold fission for the isotopic family of the most recent SHE detected of Z=115 and for the isotopic family of the already consolidated SHE of Z=111 are presented.

PACS number(s): 23.60.+e, 23.70.+j, 25.85.Ca

The first papers reporting on superheavy elements calculations were published during the 60's [1–4]. However, the experimental exploration of this area became more intense during the last decade, and the detection of superheavy nuclei has been reported in the last few years [5,6]. Recently, the superheavy nuclei $^{287}115_{172}$ and $^{288}115_{173}$ have been detected [7]. From the theoretical point of view, the extension of the Periodic Table towards the superheavy "island of stability" is very important for testing and developing nuclear structure models, as one can see in Ref. [8]. An excellent review article on superheavies can be found in Ref. [9].

The half-lives of different radioactive decay modes such as alpha decay, cluster radioactivity, and fission are important to identify the decay chains of SHE, which are the experimental signature of their formation in fusion reactions.

A simple theoretical approach has been proposed by Singh *et al.* [10] to study the cluster decay of some heavy and super-heavy nuclei (see also Refs. [11] and [12]). The proposed model is based on the fragmentation theory [13] and on the preformed cluster decay model proposed by Gupta and Malik [14]. Nuclear lifetimes for cluster radioactivity of SHE and nuclei far off the β-stability line (Z = 52-122) have been calculated in a pioneer work by Ponearu *et al.* [15].

In the present work we applied the Effective Liquid Drop Model (ELDM), which has been already used very successfully in the prediction of half-life-values of hadronic decay modes of a number of nuclei [16–22] to predict the alpha-decay, cluster emission, and cold fission half-life-values for nuclei in the region of SHE. Within the ELDM context the Coulomb and surface energies for the dinuclear shapes have been calculated analytically, thus obtaining the barrier penetrability factor for a range of mass asymmetry covering all these processes. Shell effects have been included via Q-values of the corresponding decay case, where the mass-values of the participating nuclei have been taken from Ref. [23]. The emission process is characterized by a molecular-like phase, where the daughter and emitted partners are overlapping. In this situation, two extreme descriptions for the mass transfer between the spherical fragments are considered in the literature, namely, the Varying Mass Asymmetry Shape (VMAS) and the Constant Mass Asymmetry Shape (CMAS).

These two descriptions have been already detailed in Refs. [17–20,22,25]. Gamow's penetrability factor [26] can be calculated by considering two different inertia coefficients: Werner-Wheeler's [27] and effective inertia coefficients [17]. In this work we have used the VMAS mass transfer and Werner-Wheeler's inertia coefficients. In table A of Ref. [21] one can find the numerical values of the two free model parameters used for the different nuclear decay modes of heavy nuclei.These values are being applied here to nuclei of the superheavy elements region.

At this point, we wish to emphasize the effetive character of the potential barrier of the ELDM. Accordingly, for the surface potential energy we have introduced an effective surface tension, $\sigma_{\rm eff}$, to the system in the molecular-like phase, defined through the equation

$$\frac{3}{5}e^2\left[\frac{Z_p^2}{R_p}-\frac{Z_1^2}{\bar{R}_1}-\frac{Z_2^2}{\bar{R}_2}\right]+4\pi\sigma_{\rm eff}(R_p^2-\bar{R}_1^2-\bar{R}_2^2)=Q, \tag{1}$$

where Z_ie ($i=p$, 1, 2) are the nuclear charges, respectively, of the parent, emitted, and daughter nuclei. The final radii of the fragments should be given by

$$\overline{R}_i=\left(\frac{Z_i}{Z_p}\right)^{1/3}R_p, \qquad i=1,2 \tag{2}$$

to be consistent with the uniform charge distribution considered in the Coulomb potential. The radius of the parent nucleus is determined by the simple formula

$$R_p=r_0A_p^{1/3} \tag{3}$$

where r_0 is the most significant free parameter of the model (see Table A of Ref. [21]). We remark that this definition for the surface tension establishes the effective character of the model because the difference between the energies of the initial and final configurations of the system reproduces the energy released in the disintegration, the Q-value. Therefore, for the surface potential energy we have

$$V_s=\sigma_{\rm eff}(S_1+S_2). \tag{4}$$

Here S_1 and S_2 denote the surfaces of the emitted and daughter nuclei, respectively. Another important point to remark is that although the model has been developed under the

approximattion of spherical fragments, the effect of deformation has been partially taken into account in the height of the barrier, through the Q-value of the reaction and the effective separation of the fragments at contact, which is dictated by the nuclear radius parameter, r_0. For cold fission cases, the influence of a possible, actual quadrupole deformation of fragments on the height of the barrier is certainly important, and it should, on a time, be incorporated explicitly into the present ELDM. The effect of the prolate deformation of fragments, for instance, is to lower the fission barrier at the contact configuration, therefore changing substantially (perhaps by a few orders of magnitude) the half-life of the cold fissioning system. The somewhat high value of $r_0 = 1.39$ fm used throughout the present cold fission half-life calculation is an attempt to overcome the difficult of the model in dealing with the actual fragment deformation. As it was done in Ref. [21], the cold fission and cluster emission processes are distinguished by their degree of mass asymmetry. By defining the mass asymmetry coefficient as

$$\eta = \frac{A_2 - A_1}{A_2 + A_1}, \tag{5}$$

where $A_1$and A_2 ($A_2 > A_1$) are the two fragments mass number, we have defined the cold fission process as the nuclear binary decay mode such that $\eta < 0.25$, while for $\eta > 0.25$ the process is as a cluster emission decay mode. Due to the different mass asymmetry mode involved in both cases we defined the total cold fission half-life, τ_{cf}, such that

$$\frac{1}{\tau_{cf}} = \sum_m \frac{1}{\tau_m}, \tag{6}$$

with m covering all events of $\eta < 0.25$. The cluster emission half-life, τ_{ce}, is

$$\frac{1}{\tau_{ce}} = \sum_m \frac{1}{\tau_m}, \tag{7}$$

with m covering all events of $\eta > 0.25$. The total nuclear half-life, considering the three hadronic decay modes is given by

$$\frac{1}{\tau_C} = \frac{1}{\tau_\alpha} + \frac{1}{\tau_{ce}} + \frac{1}{\tau_{cf}}. \tag{8}$$

We have performed the calculations in the region of the ZN plane defined by $155 \leq N \leq 220$ and $110 \leq Z \leq 135$. In fig.1 we show the results obtained for the alpha-decay

half-life values (top) and for the total nuclear half-life values (bottom) as a function of the proton and neutron numbers (intervals of 3.5 units of the decimal logarithm of the half-life expressed in second). We note that the alpha-decay mode is the dominant mode of decay among the three nuclear processes considered. In figures 2-5 we show the decimal logarithm of calculated half-life-values vs. neutron number for each isotopic family with Z between 110 and 133. For lower Z-values (Figs. 2 and 3), we note a local minimum around N=184 which may be associated with the possible occurrence of a spherical neutron shell closure at N=184. Since deformation effects have not been fully included in the ELDM, no typical trend around the deformed shell at N=162 should be seen for $Z > 113$. This is because the mass predictions by Möller et al [23] may not be totally reliable for nuclei of higher values of Z and A. We recall that shell effects are incorporated into the ELDM by means of the Q-value for decay obtained from the mass formula used in the calculation [23]. In Fig. 6 it is shown the half-life values for the three decay modes of SHE for the isotopic family with Z=111 (part (a)) and for the isotopic family of the most recent case of SHE detected (Z=115, part (b)). Note that the half-life-values for alpha-decay are smaller (by various orders of magnitude) than the half-lives for the other two processes, therefore being alpha decay the dominant decay mode as shown in Fig 1. It is important to mention that the present calculated half-life-values for the cold fission process are greater than those we can find in Ref. [24], because this latter work considers the ordinary spontaneous-fission process. Spontaneous-fission exhibits a distribution, among others, of kinetic energy of the fragments. The most appropriate experimental data to be compared with ours should be exclusive in the kinetic energy of fragments, i.e., modes of nuclear break-up leading to fragments with kinetic energy very near to the Q-value. In Table 1 we show a comparison between calculated and experimental decay data for the alpha emission mode.

We remark that our theoretical predictions for the alpha decay half-lives of the recent detected cases of $168 \leq N \leq 173$ using the Q-values from Ref. [23] differ from the experimental determination by less than three orders of magnitude (see Table 1, 6^{th} column). However, if the experimental Q-values from Ref. [7] are used in the ELDM routine instead of those obtained from the mass table by Möller *et al.* [23], the resulting

calculated half-lives become closer to the experimental ones, therefore showing an excellent agreement between each other (see last column of Table 1). We recall that the present half-life predictions have been obtained under the assumptions of i) ground state to ground state alpha transitions, and ii) no centrifugal effects ($l = 0$) considered. To conclude, we expect the ELDM to be helpful in predicting, within one order of magnitude or so, the half-life for the alpha decay, cluster emission and cold fission processes half-life of superheavy elements.

In summary, we are reporting the results of ELDM for a systematic calculation of the half-life for the nuclear fragmentation modes (alpha decay, cold fission and cluster emission) in a region of the ZN-plane where superheavy elements are expected to be found.

Acknowledgments

The authors wish to thank the Brazilian agencies Conselho Nacional de Desenvolvimento Científico e Tecnológico (CNPq), Fundação de Amparo à Pesquisa do Estado de São Paulo (FAPESP), Fundação de Amparo à Pesquisa do Estado de Rio de Janeiro (FAPERJ) and Fundação de Amparo à Pesquisa do Estado da Bahia (FAPESB) for partial support. The authors would also like to thank the Centro Latinoamericano de Física (CLAF) for supporting the cooperation among the different Institutions involved. One of the authors acknowledges the DAAD and TWAS for supporting part of this work.

TABLE I. Comparison between experimental results and ELDM predictions. All data presented in this table are referred to the α decay mode.

Isotope	Experimental[a]		Calculated, ELDM					
	Half-life (ms)	Q-value (MeV)	Half-life (ms)	Q-value[b] (MeV)	δ[c]	Half-life (ms)	Q-value[a] (MeV)	δ[c]
$^{288}115$	87^{+105}_{-30}	10.61±0.06	1.07×10^3	10.13	-1.1	5.19×10^1	10.61	0.2
$^{284}113$	$\left(0.48^{+0.58}_{-0.17}\right) \times 10^3$	10.15 ± 0.06	2.11×10^5	9.15	-2.6	2.12×10^2	10.15	0.4
$^{280}111$	$\left(3.6^{+4.3}_{-1.3}\right) \times 10^3$	9.87±0.06	5.51×10^1	10.14	1.8	2.96×10^2	9.87	1.1
$^{287}115$	32^{+155}_{-14}	10.74 ± 0.09	5.12×10^2	10.25	-1.2	2.48×10^1	10.74	0.1
$^{283}113$	100^{+490}_{-45}	10.26 ± 0.09	4.71×10^4	9.36	-2.7	1.10×10^2	10.26	0.0
$^{279}111$	170^{+810}_{-80}	10.52 ± 0.16	5.62×10^{-1}	10.93	2.5	5.60×10^0	10.52	1.5

[a] From Ref. [7].

[b] From Ref. [23].

[c] $\delta = \log_{10}\left(\frac{\tau_{\rm exp}}{\tau_{\rm cal}}\right)$, where $\tau_{\rm exp}$ is the experimental half-life ($2^{\rm nd}$ column), and $\tau_{\rm cal}$ is the calculated one ($4^{\rm th}$ and $7^{\rm th}$ columns).

FIGURE CAPTIONS

Fig. 1. Color diagram for the decimal logarithm of the calculated alpha-decay half-life (top) and total half-life (botton). The scale at right indicates the half-life ranges.

Fig. 2. Decimal logarithm of calculated total half-life in second vs neutron number for Z=110 to Z=115.

Fig. 3. The same as in Fig2. for Z=116 to Z=121.

Fig. 4. The same as in Fig2. for Z=122 to Z=127.

Fig. 5. The same as in Fig2. for Z=128 to Z=133.

Fig. 6. Decimal logarithm of total half-life-values for alpha decay (squares), cluster radioactivity (circles), and cold fission(triangles) decay modes vs. neutron number for Z=111 (top) and Z=115 (bottom). For clarity, only results for even-neutron isotopes are shown (quite similar result is seen for odd-neutron isotopes).

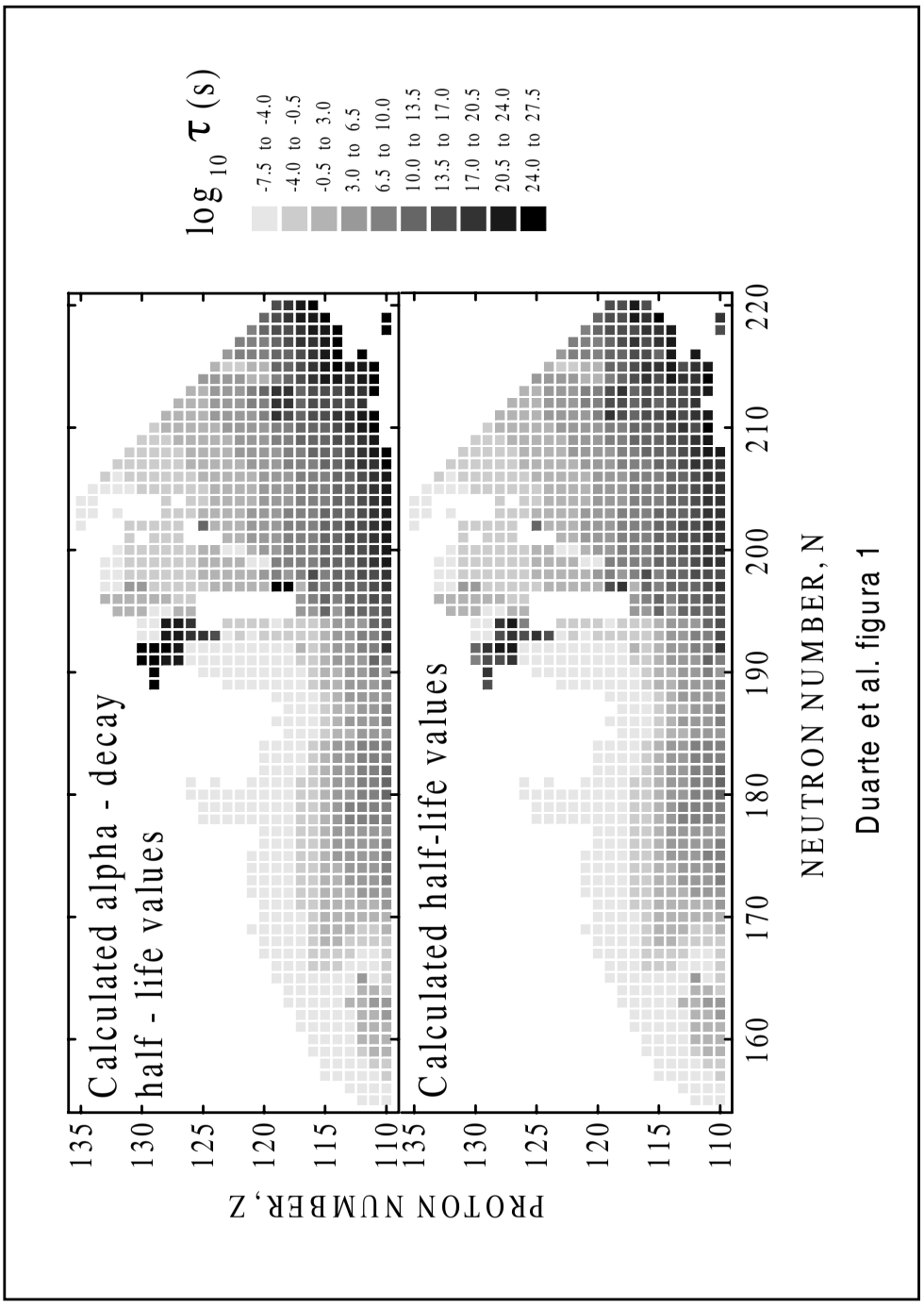
log 10 τ (s)
-7.5 to -4.0
-4.0 to -0.5
-0.5 to 3.0
3.0 to 6.5
6.5 to 10.0
10.0 to 13.5
13.5 to 17.0
17.0 to 20.5
20.5 to 24.0
24.0 to 27.5
Calculated alpha - decay
half - life values
Calculated half-life values
PROTON NUMBER, Z
NEUTRON NUMBER, N
135
130
125
120
115
110
160
170
180
190
200
210
220
Duarte et al. figura 1

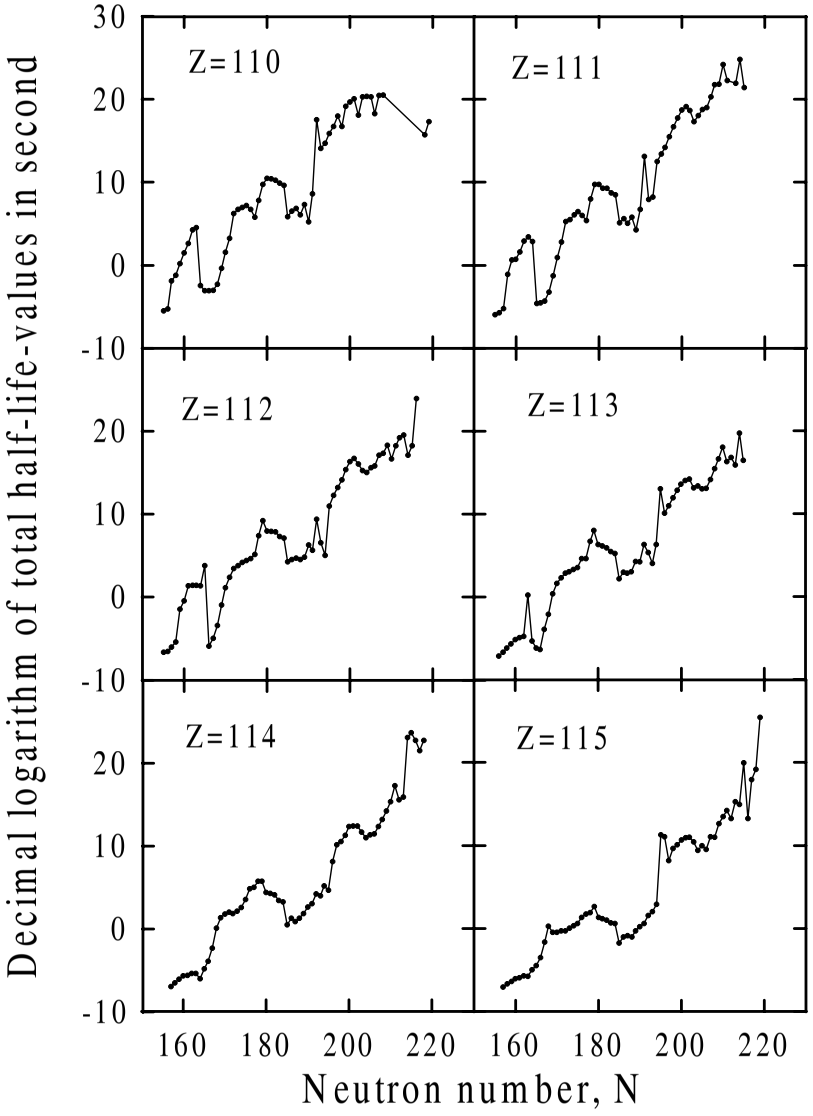

Duarte, et al. Fig. 2

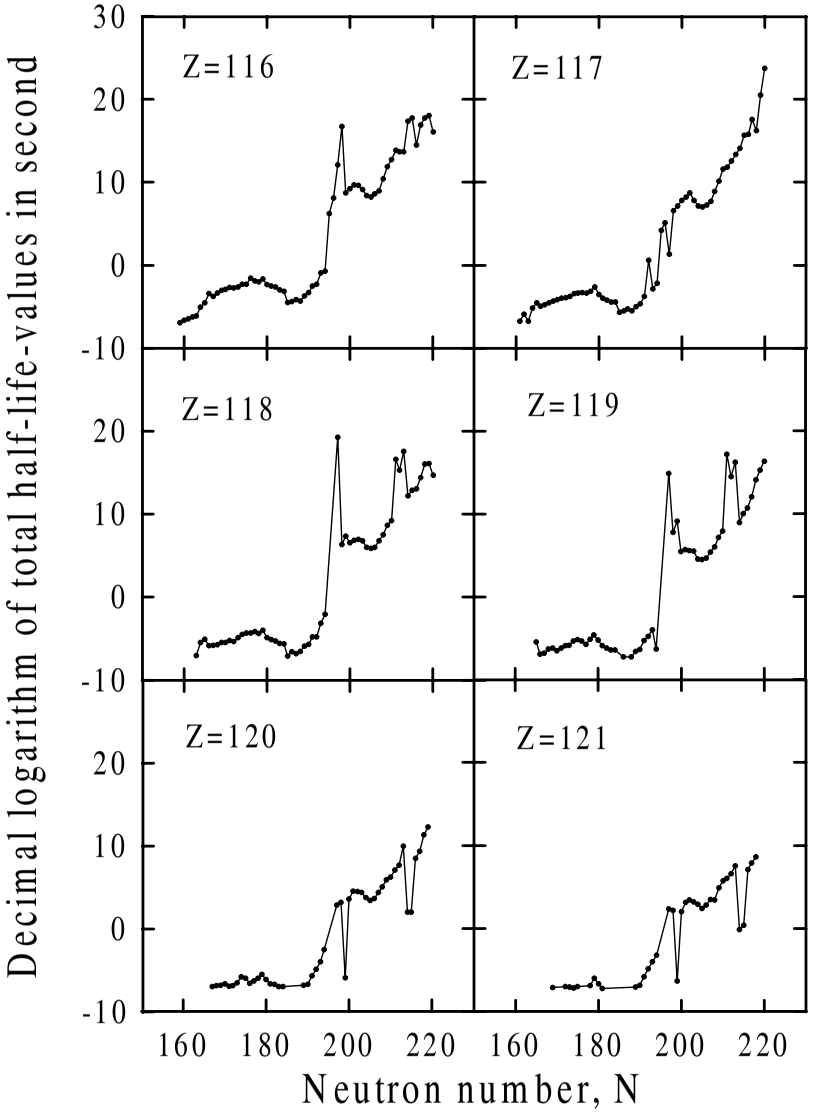

Duarte et al, Fig. 3

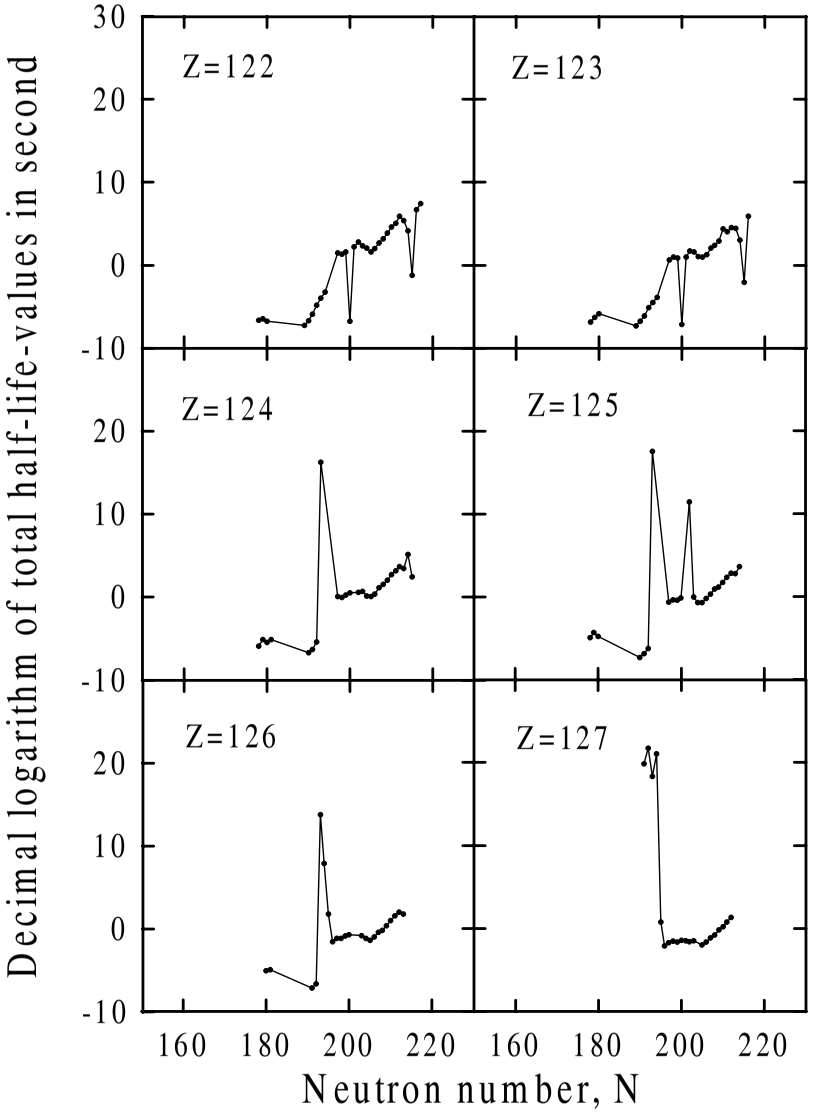

Duarte et al Fig 4

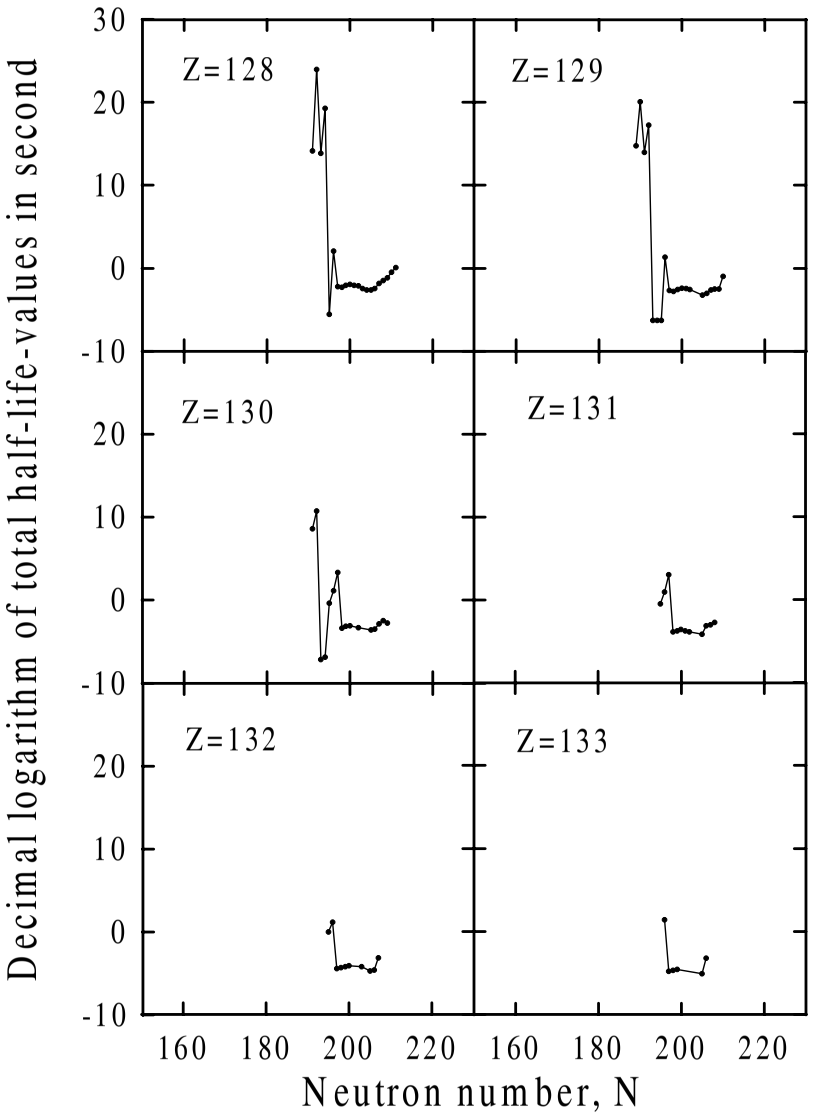

Duarte et al Fig. 5

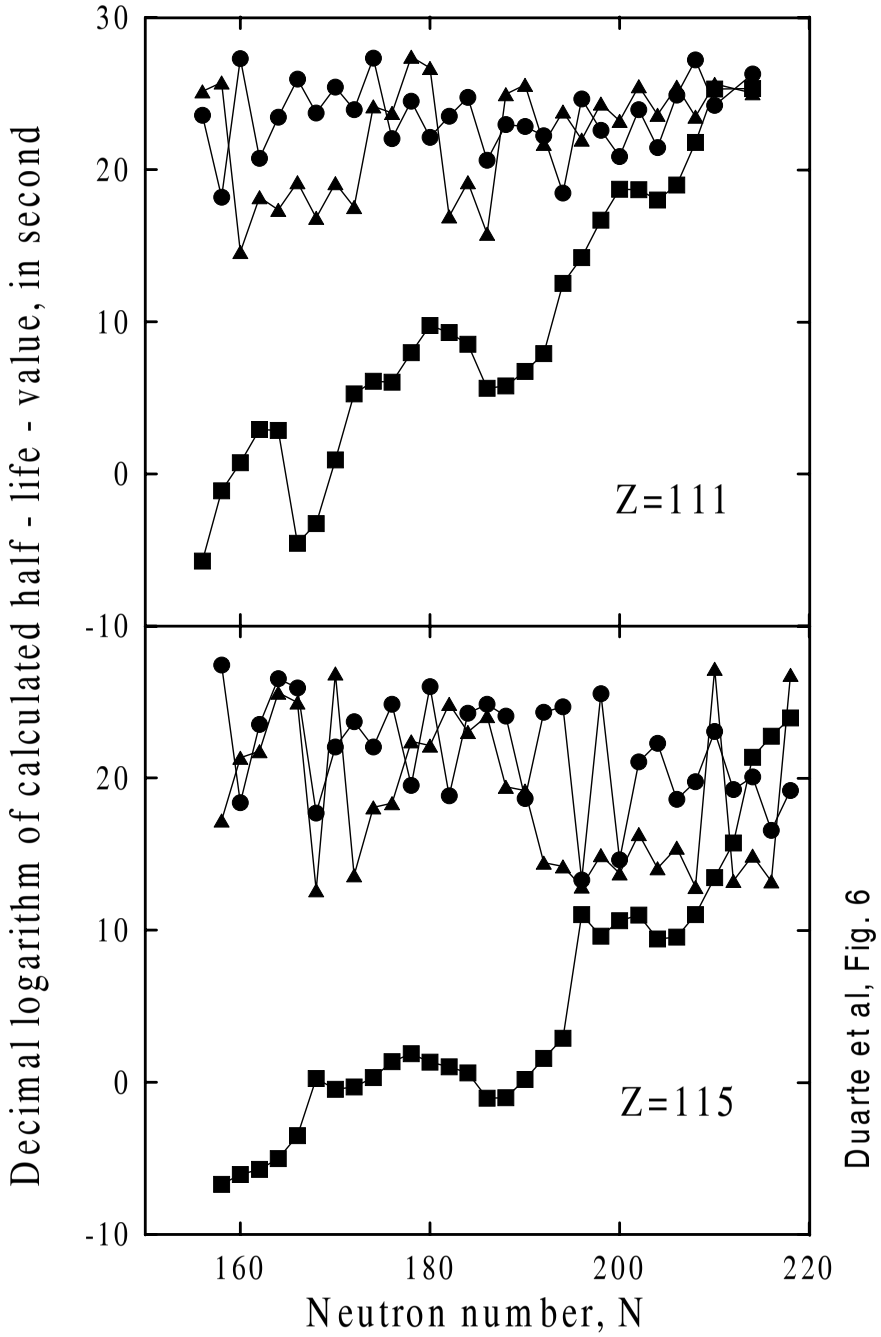
Decimal logarithm of calculated half - life - value, in second
30
20
10
0
-10
Z=111
20
10
0
-10
Z=115
160
180
200
220
Neutron number, N
Duarte et al, Fig. 6

REFERENCES

[1] W. D. Myers and W. J. Światecki, Nucl. Phys. **81**, 1 (1966).

[2] H. Meldner, in *Proceedings of the International Symposium on Nuclides far off the Stability Line,* Lysekil, Sweden, August 21-27 (1966), edited by W. Forsling, C. J. Herrlander, and H. Ryde, Ark. Fys. **36**, 593 (1967).

[3] S. G. Nilsson, J. R. Nix, A. Sobiczewski, Z. Szymansky, S. Wycech, C. Gustafson, and P. Möller, Nuc. Phys. A **115**, 545 (1968).

[4] U. Mosel and W. Greiner, Z. Phys. **222**, 261 (1969).

[5] Yu. Ts. Oganessian, V. K. Utyonkoy, Yu. V. Lobanov, F. Sh. Abdullin, A. N. Polyakov, I. V. Shirokovsky, Yu. S. Tsyganov, G. G. Gulbekian, S. L. Bogomolov, B. N. Gikal, A. N. Mezentsev, S. Iliev, V. G. Subbotin, A. M. Sukhov, G. V. Buklanov, K. Subotic, M. G. Itkis, K. J. Moody, J. F. Wild, N. J. Stoyer, M. A. Stoyer, and R. W. Lougheed, Phys. Rev. Lett. **83**, 3154 (1999).

[6] Yu. Ts. Oganessian, A. V. Yeremin, A. G. Popeko, O. N. Malyshev, and A. B. Yakushev, J. Nucl. Radioch. Sci. **3**, 217 (2002).

[7] Yu. Ts. Oganessian, V. K. Utyonkoy, Yu. V. Lobanov, F. Sh. Abdullin, A. N. Polyakov, I. V. Shirokovsky, Yu. S. Tsyganov, G. G. Gulbekian, S. L. Bogomolov, A. N. Mezentsev, S. Iliev, V. G. Subbotin, A. M. Sukhov, A. A. Voinov, G. V. Buklanov, K. Subotic, V. I. Zagrebaev, M. G. Itkis, J. B. Patin, K. J. Moody, J. F. Wild, M. A. Stoyer, N. J. Stoyer, D. A. Shaughnessy, J. M. Kenneally and R. W. Lougheed, Phys. Rev. C **69**, 021601(R) (2004).

[8] V. Yu. Denisov and S. Hofmann, Phys. Rev. C **61**, 034606 (1999).

[9] S. Hofmann and G. Münzenberg, Rev. Mod. Phys. **72**, 733 (2000).

[10] S. Singh, R. K. Gupta, W. Scheid, and W Greiner, J. Phys. G: Nucl. Part. Phys. **18**, 1243

(1992).

[11] Raj K. Gupta, Sarbjit Singh, Rajeev K. Puri, and Werner Scheid, Phys. Rev. C **47**, 561 (1992).

[12] Raj K. Gupta, Sarbjit Singh, Gottfried Münzenberg, and Werner Scheid, Phys. Rev. C **51**, 2623 (1995).

[13] H. J. Fink, J. A. Marhun, W. Scheid and W. Greiner, Z. Phys. **268** 321 (1974).

[14] S. S. Malik, S. Singh, R. K. Puri, S. Kumar and R. K. Gupta, Pramana J. Phys. **32**, 419 (1989).

[15] D. N. Poenaru, D. Schnabel, W. Greiner, D. Mazilu and R. Gherghescu, At. Data Nucl. Data Tables. **48**, 231 (1991).

[16] M. Gonçalves and S. B. Duarte, Phys. Rev. C **48**, 2409 (1993).

[17] S. B. Duarte and M. Gonçalves, Phys. Rev. C **53**, 2309 (1996).

[18] S. B. Duarte, M. Gonçalves and O. A. P. Tavares, Phys. Rev. C **56**, 3414 (1997).

[19] S. B. Duarte, O. Rodríguez, O. A. P. Tavares, M. Gonçalves, F. García, and F. Guzmán, Phys. Rev. C **57**, 2516 (1998).

[20] O. A. P. Tavares, S. B. Duarte, O. Rodríguez, F. Guzmán, M. Gonçalves and F. García, J. Phys. G: Nucl. Part. Phys. **24**, 1757 (1998).

[21] S. B. Duarte, O. A. P. Tavares, F. Guzmán, A. Dimarco, F. García, O. Rodríguez and M. Gonçalves, At. Data and Nuc. Data Tables **80**, 235 (2002).

[22] O. Rodríguez, F. Guzmán, S. B. Duarte, O. A. P. Tavares, F. García and M. Gonçalves, Phys. Rev. C **59**, 253 (1999).

[23] P. Möller, J. R. Nix, W. D. Myers and W. J. Swiatecki, At Data Nuc. Data Tables. **59**, 185 (1995).

[24] R. Smolańczuk, J. Skalski, and A. Sobiczewski, Phys. Rev. C **52**, 1871 (1995).

[25] M. Gonçalves, S. B. Duarte, F. García, and O. Rodríguez, Comput. Phys. Commun. **107**, 246 (1997).

[26] G. Gamow, Z. Phys. **51**, 204 (1928).

[27] D. N. Ponearu, J. A. Marhun, W. Greiner, M. Ivascu D. Mazilu, and I. Ivascu, Z. Phys. A **333**, 291 (1989).